Decomposition of the magnetoresistance of multilayers into ferromagnetic and superparamagnetic contributions

I. Bakonyi,* L. Péter, Z. Rolik,† K. Kiss-Szabó,† Z. Kupay,† J. Tóth, L. F. Kiss, and J. Pádár
Research Institute for Solid State Physics and Optics, Hungarian Academy of Sciences, H-1525 Budapest, P.O.B. 49, Hungary
(Received 2 March 2004; revised manuscript received 10 May 2004; published 31 August 2004)

An analysis of both magnetic and magnetotransport properties is presented for electrodeposited multilayers prepared intentionally under conditions to make the superparamagnetic (SPM) magnetization contribution comparable to or larger than the ferromagnetic term. Based on a model elaborated for the giant magnetoresistance (GMR) of granular metals [N. Wiser, J. Magn. Magn. Mater. **159**, 119 (1996); B. Hickey *et al.*, Phys. Rev. B. **51**, 667 (1995)], it is shown that in such multilayers both the magnetization and the GMR can be decomposed into ferromagnetric and superparamagnetic contributions where the latter term is described by a Langevin function. The size of the SPM regions estimated from the experimental data is in the nanoscale regime. It is believed that the method applied here gives a quantitative answer to the problem of the often observed nonsaturating behavior of GMR in multilayers. Electrodeposited multilayers are particularly prone to this feature although the occurrence of SPM regions is quite common in multilayers prepared by any technique. Therefore, this type of analysis should help better understanding of the factors influencing the GMR of multilayer films.

DOI: 10.1103/PhysRevB.70.054427 PACS number(s): 75.47.De, 75.70.Cn, 75.20.−g, 81.15.Pq

I. INTRODUCTION

It has been reported for several magnetic/nonmagnetic multilayer systems that the magnetoresistance (MR) can exhibit a strongly nonsaturating behavior,[1–25] sometimes up to magnetic fields of several tens of kOe. Since the saturation against an antiferromagnetic (AF) coupling in multilayers can usually be achieved in a few kOe,[26–28] this nonsaturating MR component should have a different origin. Magnetic measurements have often revealed[7,12,15,17,18,21,23,29,30] that in multilayers, in addition to the ferromagnetic (FM) term, the magnetization also has a superparamagnetic (SPM) term, the latter one sometimes even dominating over the FM contribution. The phenomenon of nonsaturating magnetoresistance and the occurrence of a SPM magnetization contribution are not restricted to any specific deposition technique or element combination since, depending on layer thicknesses and specific deposition conditions, it has been observed in multilayers of the Co/Au, Co/Cu, Ni/Cu, Ni-Fe/Cu, and Ni-Co/Cu systems grown by various methods such as molecular-beam epitaxy (MBE), sputtering, or electrodeposition.

Due to the possible occurrence of SPM behavior in multilayers, it is tempting to ascribe the nonsaturating MR to the presence of SPM regions. This was performed first for MBE-grown Co/Cu multilayers[3,4] by fitting the magnetic field dependence of the MR(H) curves by a Langevin function $L(x)$ known to describe the magnetization of SPM entities where $x=\mu H/kT$ with μ as the magnetic moment of the SPM particles.[31] A similar analysis has recently been performed for electrodeposited Ni-Co-Cu/Cu multilayers.[19]

Although the MR behavior for these multilayers could be successfully described in the form $\mathrm{MR}(H) \propto L(x)$, a theoretical justification of such an empirically found field dependence of the magnetoresistance is also needed. Namely, in granular metals containing noninteracting SPM particles embedded in a nonmagnetic matrix, the magnetoresistance was predicted to follow the relation $\mathrm{MR}(H) \propto [L(x)]^2$ (Refs. 32 and 33) and this behavior was, indeed, observed experimentally in many cases.[34,35]

A significant progress has been achieved by establishing that in multilayers with nonsaturating MR behavior the observed magnetoresistance can be ascribed to the presence of both FM and SPM regions which were revealed by simultaneous magnetization measurements over a wide temperature range.[12,23] Namely, by recognizing that the magnetic layers contain both FM and SPM regions, one can apply the model developed by Wiser and Hickey and their co-workers[36,37] for granular metals. This model was elaborated to explain the field dependence of the magnetoresistance for some granular alloys which did not obey the $\mathrm{MR}(H) \propto [L(x)]^2$ relation. It was assumed that for a given temperature there is a distribution of magnetic particle sizes with some particles being in the SPM regime and the rest of the particles in the FM regime. In terms of the Wiser-Hickey model,[36,37] in the simultaneous presence of both FM and SPM regions the GMR can contain three contributions: (i) $\mathrm{GMR}_{\mathrm{SPM\text{-}SPM}}$, (ii) $\mathrm{GMR}_{\mathrm{FM\text{-}FM}}$, and (iii) $\mathrm{GMR}_{\mathrm{SPM\text{-}FM}}(=\mathrm{GMR}_{\mathrm{FM\text{-}SPM}})$, whereby a term $\mathrm{GMR}_{A\text{-}B}$ means a spin dependent scattering event for an electron path "magnetic region $A \rightarrow$ nonmagnetic region $\rightarrow$ magnetic region B."

Each of these three cases makes a completely different contribution to the field dependence of the magnetoresistance MR(H) since for a SPM particle, a large magnetic field (typically well in excess of 10 kOe) is needed to align its magnetic moment whereas the moment of a FM particle is aligned in a much smaller magnetic field, typically in a few kOe. Case (i) corresponds to a conventional granular metal with SPM particles only for which $\mathrm{MR}(H) \propto [L(x)]^2$.[32,33] For case (ii), the moments of both FM particles are aligned at relatively small fields and the magnetic field has then no further effect on the resistivity. Therefore, scattering along an

electron path "FM particle 1 → nonmagnetic region → FM particle 2" does not contribute to the MR above the relatively small saturation field of the FM particles. For case (iii), i.e., for an electron path "SPM particle → nonmagnetic region → FM particle" or "FM particle → nonmagnetic region → SPM particle," since the moment of the FM particle is aligned at its small saturation field, for higher magnetic fields the correlation of the two magnetic moments involved depends on the time average of the spatial orientation of the SPM particle moment only. This was shown[36,37] to lead to a linear dependence of the magnetoresistance on the SPM magnetization for high fields, i.e., $\mathrm{MR}(H) \propto L(x)$. The above discussed results[36–40] refer to an extension of conventional granular alloys containing SPM particles only to the case when FM particles are also present. The aim of the present paper is to show that in some cases the conventional picture of magnetic/nonmagnetic multilayers with purely FM layers only should be extended in the opposite way, i.e., by accounting also for the presence of SPM regions.

For this purpose, a detailed room-temperature study of electrodeposited Co-Cu/Cu multilayer samples will be presented on the basis of taking into account, in addition to a FM contribution, a SPM term as well. Special emphasis will be devoted to comparing the results of analyses of the magnetic field dependence for both the magnetization and magnetoresistance for a given sample. An important aim of this work is to demonstrate that by such an analysis the observed MR can be reasonably well separated into a FM and a SPM contribution. The quantitative analysis allows us to determine the magnitude of the GMR contribution which arises due to spin-dependent scattering processes involving SPM regions. The multilayer samples selected for the current study were *intentionally* prepared under electrochemical conditions allowing the formation of a large SPM fraction of the magnetic layer. The purpose of this choice was to allow a clear demonstration of the possibility of separating the FM and SPM contributions, by making the latter one to be significant, or even dominant.

It turned out from the quantitative analysis that beyond the technical saturation of the FM component at about 1.7 kOe, the field dependence of both the magnetization and the GMR can be described by the Langevin function $L(x)$. In terms of the Wiser-Hickey model,[36,37] this means that in these Co-Cu/Cu multilayers the GMR arises from spin-dependent scattering of electrons which travel through the nonmagnetic spacer between two FM regions ($\mathrm{GMR_{FM}}$) or between a FM region and a SPM region ($\mathrm{GMR_{SPM}}$) whichever is the first or second where we introduced simplified notations for the $\mathrm{GMR_{FM\text{-}FM}}$ and $\mathrm{GMR_{SPM\text{-}FM}} = \mathrm{GMR_{FM\text{-}SPM}}$ terms, respectively. Accordingly, we can visualize the magnetic layers in the present multilayers as being broken up into FM and SPM regions due to the specific deposition conditions and the SPM regions are decoupled from the FM regions of the magnetic layers.

The paper is organized as follows. In Sec. II, the details of sample preparation and investigations are described. Sections III and IV present the results of magnetic and MR measurements, respectively, including a quantitative decomposition of both measured properties into FM and SPM contributions. Finally, a summary is given in Sec. V.

II. EXPERIMENTAL

A. Sample preparation

An aqueous electrolyte with two solutes ($CoSO_4$ and $CuSO_4$) was used to prepare magnetic/nonmagnetic Co-Cu/Cu multilayers by the usual pulse plating technique under galvanostatic control in an arrangement described in Ref. 16. A polished polycrystalline Ti sheet in vertical position served as cathode. The Co-Cu/Cu multilayers were deposited in the form of 20 mm × 20 mm square shaped foils with a typical total thickness of several micrometers. The multilayer deposits were removed from their substrates by mechanical stripping.

It turned out from our previous study on electrodeposited Co-Cu/Cu multilayers prepared by pulse plating[16] that even if the amplitude of the second current pulse is set to zero or to a small positive (anodic) value, sufficiently thick nonmagnetic Cu layers can build up between the magnetic Co-rich layers. A structural study by x-ray diffraction on a sample prepared with zero current for the second pulse[16] has indeed revealed the presence of superlattice reflections due to the composition modulation and the structure is expected to be similar also for small anodic currents during the second pulse. The magnitude of the observed GMR was only slightly reduced with respect to multilayers prepared by cathodic Cu deposition pulses, again substantiating the formation of a Cu (or Cu-rich) nonmagnetic layer between the Co-rich magnetic layers.

The explanation for this phenomenon is the so-called exchange reaction[41,42] which involves a dissolution of the previously deposited less noble Co atoms and a simultaneous deposition of the more noble Cu atoms. The Cu dissolution and Co deposition by the exchange reaction takes place randomly over the cathode area but the net current due to this process is zero. When the cathodic current during the Cu deposition pulse is lower than the mass transport limited Cu deposition current, the Cu^{2+} ions at the deposit surface are only partly used for Cu deposition assisted by the external current source. The leftover Cu^{2+} ions spontaneously oxidize the previously deposited Co-rich layer ($Cu^{2+} + Co = Cu + Co^{2+}$). The exchange reaction also takes place when the current is zero or exhibits such a small anodic value that does not lead to Cu dissolution instead of Cu deposition. The formation of a fairly thick spacer layer during galvanostatic pulse plating due to the exchange reaction has been demonstrated for Ni-Cu/Cu multilayers as well which were prepared with zero Cu deposition current and in which a clear GMR effect could be observed.[14,20,24]

For the present Co-Cu/Cu multilayers, a cathodic current pulse of $-32.5\ \mathrm{mA/cm^2}$ amplitude and 0.65 s duration was applied to deposit a magnetic layer which resulted in a nominal thickness of 6.8 nm.[16] Two multilayer samples were selected for the current study which were prepared at $+0.5\ \mathrm{mA/cm^2}$ anodic current density of the Cu deposition with pulse duration $t_{\mathrm{Cu}} = 2$ s (sample No. 2) and $t_{\mathrm{Cu}} = 3$ s (sample No. 3). The repetition number of the cathodic/anodic pulse combination was 1144 and 1325 for sample No. 2 and No. 3, respectively.

It has been reported[16,20] that in the case of electrodepositing multilayers on a vertical substrate, there is a substantial

TABLE I. Results of chemical composition analysis and individual layer thicknesses estimated from the composition data.

Sample strip		overall Co content (at.%)	Co-rich layer thickness (nm)	Cu layer thickness (nm)
Name	Type			
2A	multilayer	72±8	5.0±0.6	1.6±0.6
2B	multilayer	60±5	4.2±0.4	2.4±0.4
3A	multilayer	68±2	4.6±0.1	1.9±0.1
3B	multilayer	55±9	3.8±0.6	2.7±0.6
CoA	bulk Co-Cu alloy	94±0.6		
CoB	bulk Co-Cu alloy	92±2		

variation of the MR properties along the vertical direction. Therefore, we have cut about 2 mm wide horizontal strips out of both multilayer foils Nos. 2 and 3. One strip was cut at positions between 2 and 4 mm (strip A) and another one between 12 and 14 mm (strip B), with the positions measured from the top edge of the deposit. In this manner, we had altogether four horizontally cut, 2 mm wide multilayer strips (Nos. 2A, 2B, 3A, and 3B). For comparison, a Co-rich Co-Cu bulk magnetic alloy foil has also been electrodeposited from the same bath by direct-current plating at the same current density as the magnetic layer in the multilayers, i.e., with the same chemical composition. Similarly to the multilayers, 2 mm wide horizontal strips were cut at the same positions (between 2 and 4 mm and 12 and 14 mm) and these will be denoted as strips CoA and CoB, respectively.

B. Composition analysis and layer thickness estimates

Chemical analysis was performed by electron probe microanalysis (EPMA) by using a RÖNTEC microsonde equipment and evaluation software in a JEOL 840 SEM electron microscope. The composition analysis results are summarized in Table I. The relative accuracy (reproducibility) of the chemical analysis for the combination of Co and Cu is about ±0.2 at. %. The larger scatter of the results in Table I reflects, therefore, actual lateral variations of the composition. Along the horizontal strips, the Co content was systematically higher towards the ends due to an increased deposition current density there (so-called "edge effect").

The data in Table I reveal that the Co content in the multilayers is much smaller than in the bulk Co-Cu deposits (strips CoA and CoB). This is just evidence that a large fraction of the Co atoms deposited during the cathodic pulse dissolves due to the Co to Cu exchange process taking place with such an efficiency that finally a Cu layer is built up betweeen the magnetic layers. For a given position (A or B), the Co-content reduction is stronger for $t_{Cu}=3$ s (strips of sample No. 3) than for $t_{Cu}=2$ s (strips of sample No. 2). This result is a direct consequence of the different t_{Cu} times until the exchange reaction was allowed to take place. The much larger scatter of the multilayer analysis results with respect to the bulk alloy data can be explained by the fact that the exchange reaction takes place randomly over the cathode area and, therefore, the amount of dissolved Co/deposited Cu more strongly fluctuates laterally in the multilayer.

As in our previous studies,[22,41] we can calculate the individual layer thicknesses from the result of composition analysis by taking into account that the magnetic layer composition is equal to the bulk alloy composition at the same position (*A* or *B*) and the nonmagnetic layer formed due to the exchange reaction consists of pure Cu. The calculated average thicknesses are specified in Table I. The large lateral composition variations due to the random nature of the exchange reaction also lead to large fluctuations of the layer thicknesses around the average effective value. Nevertheless, e.g., for strip No. 3B nearly half of the magnetic layer was converted into a Cu spacer layer by the exchange reaction.

C. Magnetoresistance and magnetic measurement techniques

The MR was measured on the strips at room temperature with the four-point-in-line method in magnetic fields between −8 kOe and +8 kOe in the field-in-plane/current-in-plane geometry. Both the longitudinal (LMR) and the transverse magnetoresistance (TMR) (field parallel to current and field perpendicular to current, respectively) components were recorded for each sample. The following formula was used for calculating the magnetoresistance ratio: $\Delta R/R_0=[R(H)-R(0)]/R(0)$ where $R(H)$ is the resistance in the magnetic field H and $R(0)$ is the resistance when $H=0$. A vibrating sample magnetometer (VSM) was used to measure the in-plane magnetization curves at room temperature up to about $H=14$ kOe on the same strips as used for the MR measurements.

III. MAGNETIC PROPERTIES

The magnetization curves were measured at room temperature with descending magnetic field after saturation in $H=14$ kOe. A typical result is plotted in Fig. 1 for the multilayer strip No. 3A. The inset shows the hysteresis loop at low magnetic fields from which the coercive field H_c can be deduced.

It was observed that technical saturation of the FM contribution was reached at about $H_s=1.7$ kOe. However, Fig. 1 indicates that there is a strong variation of the magnetization up to the highest magnetic fields applied. This high-field

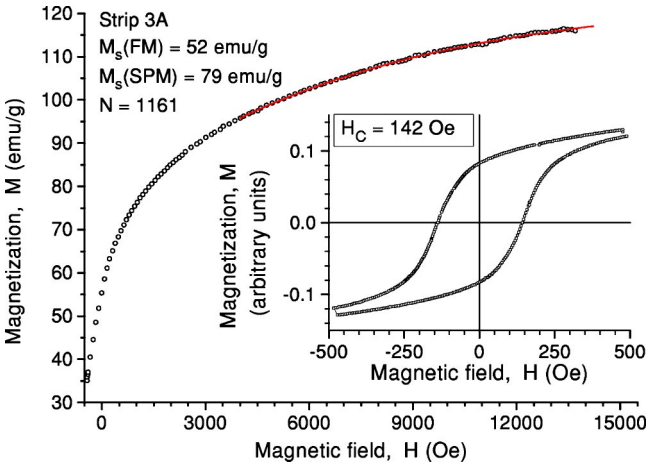

FIG. 1. Room-temperature magnetization data (o) for the multilayer strip 3A with a SPM fit (solid line) according to Eq. (1) for $H>1.7$ kOe. The fit parameter values for M_{FM}, M_{SPM}, and N_M are also displayed. The magnetization curve was measured with decreasing magnetic field after saturation at about $H=14$ kOe. The inset shows the hysteresis loop on an expanded scale and the value of the coercive field (H_c).

magnetization change originates from SPM regions in the multilayer sample. The magnetization curves for $H>H_s=1.7$ kOe could be described as

$$M(H) = M_{FM} + M_{SPM}L(x) \quad (H > H_s). \tag{1}$$

Here, M_{FM} and M_{SPM} are the room-temperature saturation magnetization values for the FM and SPM component, respectively, and $L(x)$ the Langevin function with $x=\mu H/kT$. The average magnetic moment of a SPM region is given by $\mu=N_M\mu_B$ with μ_B as the Bohr magneton and the subscript M refers to the fact that N was deduced from magnetization data. The fit of the experimental data in Fig. 1 with Eq. (1) for $H>H_s$ is displayed by the solid line, well demonstrating a SPM behavior for high magnetic fields. From the fit, the parameters M_{FM}, M_{SPM}, and N_M are deduced as given in the figure. Very similar results were obtained also for the other three multilayer strips and the fit parameters and coercive field data are collected in Table II.

The quantity N_M characterizing the average size of SPM regions does not show a systematic variation (Table II). Its value is larger for sample No. 2 with strongly different values for strips 2A and 2B whereas it is practically equal for strips 3A and 3B.

We can infer from Table II that the H_c values are about 2 to 4 times higher than for the bulk $Co_{92}Cu_8$ alloy. This comes partly from finite size effects since it has been well known for FM thin films[43] that H_c increases strongly from the bulk value with decreasing film thickness. This effect is especially pronounced if the magnetic layer thickness gets down to the nanometer range as was shown for electrodeposited Co films[44] and Co-Cu/Cu multilayers.[25] The H_c values also differ between strips A and B at a given t_{Cu} time and for both multilayers 2 and 3, we obtained $H_c(B)=1.7\ H_c(A)$.

It might be appropriate now to discuss briefly how the specific preparation conditions of the Co-Cu/Cu multilayers investigated result in the formation of SPM regions in the magnetic layers. It was discussed in Sec. II that under the deposition conditions applied an exchange reaction takes place. The effect of the exchange reaction is that due to the partial dissolution of the previously deposited magnetic layer during the anodic pulse, the actual magnetic layer thickness is reduced (and, conversely, the nonmagnetic layer thickness increases) as was shown by direct chemical analysis here and in previous works.[22,41] Since this process takes place quite randomly on the surface of the lastly deposited magnetic layer, the consequences can be either a strong chemical intermixing across the interface, a roughening of the surface/interface, a fluctuation in the individual layer thicknesses and/or the development of an undulation of the multilayer planes. In addition, the application of anodic current pulses between the cathodic pulses for the magnetic layer deposition results in a partial dissolution of the magnetic layers and this can further enchance the chemical intermixing and layer thickness fluctuations.

One important aspect of the above described electrochemical processes is that they can give rise to the formation of magnetic regions with so-called "loose moments" which

TABLE II. Magnetic parameters (saturation magnetization M and coercive field H_c) of the strips investigated. The saturation magnetization values of the ferromagnetic (M_{FM}) and superparamagnetic (M_{SPM}) components as well as parameter N_M were deduced by fitting the experimental data to Eq. (1). The last row gives the coercive field H_c for the bulk Co-Cu alloy strip CoB prepared by dc plating.

Sample strip	M_{FM} (emu/g)	M_{SPM} (emu/g)	M_{SPM}/M_{FM}	N_M	H_c (Oe)
2A Co(5.0 nm)/Cu(1.6 nm)	75	66	0.88	1387±20	114
2B Co(4.2 nm)/Cu(2.4 nm)	37	50	1.37	1846±20	215
3A Co(4.6 nm)/Cu(1.9 nm)	52	79	1.52	1162±20	142
3B Co(3.8 nm)/Cu(2.7 nm)	50	61	1.22	1153±20	239
CoB bulk $Co_{92}Cu_8$ alloy					64

are not completely coupled to the FM parts of the magnetic layers. These regions can be interfacial layers of reduced Co content with localized atomic moments or giant-moment paramagnetic clusters. In extreme cases, the random dissolution of the magnetic layer can lead to a strong fluctuation of the magnetic layer thicknesses, and can even result in the formation of magnetically isolated regions (islands) of the FM metal or alloy. Due to their nanoscale size, these islands can exhibit a SPM behavior and the data in Table II well confirm the formation of SPM regions in these particular Co-Cu/Cu multilayers. The magnitude of the SPM magnetization contribution is significant for each multilayer strip, mostly even dominating over the FM term. The M_{SPM} term is larger in sample No. 3 than in sample No. 2 at the same vertical position (*A* or *B*). This is expected since for $t_{Cu}=3$ s, the exchange reaction can act longer than for $t_{Cu}=2$ s. Also, M_{SPM} is larger for both anodic pulse lengths ($t_{Cu}=2$ and 3 s) at position *A* than at position *B*. This indicates that the deposition conditions at position *A* are more favorable for the formation of SPM regions than at position *B*.

IV. MAGNETORESISTANCE CHARACTERISTICS

The MR curves are shown at both positions *A* and *B* for samples Nos. 2 and 3 in Figs. 2(a) and 2(b), respectively. Most of these multilayer MR curves exhibit typical nonsaturating behavior. The MR($H=8$ kOe) values are negative except for the LMR component of strip 2A. For each strip, a significant splitting between the LMR and TMR components can be observed. For explaining this splitting, we have to consider first the MR curves of the bulk ferromagnetic $Co_{92}Cu_8$ alloy [strip CoB, Fig. 2(c)] which has the same chemical composition as the magnetic layer in the multilayer structure at position *B*.

In bulk homogeneous ferromagnets, the MR depends on the relative orientation of the magnetization and the measuring current.[45–47] In magnetic fields beyond technical saturation where the magnetization is already fully aligned along *H*, the difference between the LMR and TMR components of the magnetoresistance of bulk homogeneous ferromagnets is called as the anisotropic magnetoresistance AMR=LMR-TMR. Indeed, in Fig. 2(c) we can observe a constant difference LMR-TMR of about 1.9% for sample CoB in magnetic fields above 2 to 3 kOe. This AMR value is very close to those reported previously for pure Co films.[47,48] This finding implies that a few percent of Cu dissolved in Co induces minor changes only in the magnetotransport behavior of Co.

According to the data in Figs. 2(a) and 2(b), the AMR term at $H=8$ kOe is about 1.5% (2A), 1.1% (2B), 1.5% (3A), and 0.8% (3B) for the four strips investigated. In view of these AMR data and the total MR values at $H=8$ kOe [see Figs. 2(a) and 2(b)], we can establish the following: (i) strip 2A exhibits an AMR contribution nearly as large as the bulk $Co_{92}Cu_8$ alloy and a small GMR contribution shifting somewhat both the LMR and TMR components towards (more) negative values, (ii) strips 2B and 3A have very similar total MR values and the negative sign of both the LMR and the TMR components indicates the presence of a clear GMR effect on which still relatively large AMR contributions are

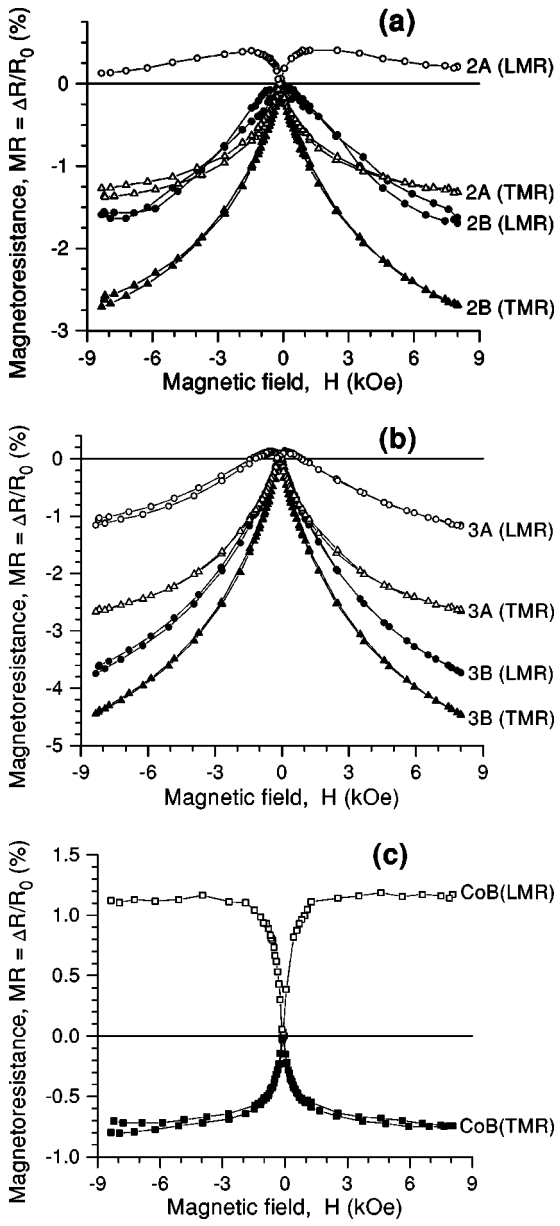

FIG. 2. Longitudinal (LMR) and transverse (TMR) magnetoresistance curves (a) for multilayer strips 2A and 2B, (b) for multilayer strips 3A and 3B, and (c) for the bulk $Co_{92}Cu_8$ alloy strip CoB.

superimposed, (iii) strip 3B has the largest total MR values in which the dominant contribution is GMR since the AMR term here is about 20% of the total MR only. The presence of significant AMR terms in these multilayers is due to the fact that the thickness of the magnetic layers is relatively large (4 to 5 nm, see Table I). In such a case, the in-plane MR of multilayers definitely contains a non-negligible contribution from successive electron scattering events within each magnetic layer and this gives rise to AMR as observed. Possible origins leading to differences in the deposition conditions between positions *A* and *B* have been discussed to some extent in Ref. 20; however, to clear up these factors in detail would require a more thorough study and this already lies beyond the scope of the present paper. Here we can note only

that apparently at position *A*, the conditions are less favorable for the Cu atoms while being deposited via the exchange reaction to form a continuous layer. Namely, the evident AMR contributions here suggest a stronger percolation of the magnetic regions and, therefore, the magnetic and MR behavior becomes more bulklike than for position B.

We can make some comments on the observed MR characteristics also in the light of the magnetic data. For strip 2A, a predominantly AMR behavior was observed. The curvature of the LMR and TMR curves is relatively small above technical saturation, indicating a large FM fraction of the magnetic layers. As Table II shows, for this sample, indeed, we have $M_{FM} > M_{SPM}$. We can explain this observation by saying that for this multilayer sample, t_{Cu} was not sufficiently high for the development of a continuous Cu layer via the exchange reaction even if the effective Cu layer thickness was estimated to be 1.6 nm (Table I). Due to the remaining pinholes in the Cu layer, direct contacts between the magnetic layers establish a FM coupling of their magnetizations.

As described above, the MR curves of the other three multilayer strips (2B, 3A, and 3B) indicated a significant GMR contribution in comparison with the AMR term. This means that here the observed MR is dominated by spin-dependent scattering processes due to a heterogeneous magnetic nanostructure in which FM coupling is not substantial. It follows that in these three multilayer strips a sufficiently thick, continuous Cu spacer layer could be built up due to the exchange reaction. Indeed, the Cu layer thicknesses estimated in Table I turned out to be as high as about 2 nm or more. The formation of such a thick Cu layer could take place by consuming a large fraction of the previously deposited magnetic layer as found also in some recent electrodeposited multilayer studies.[22,41] However, during this strong "consumption" of the magnetic layers, a larger fraction of them could be converted at the same time into SPM regions. This is again well reflected in the data of Table II which indicate M_{SPM}/M_{FM} ratios greater than 1 for all of these three multilayer strips.

In terms of the results derived from the magnetic measurements (Sec. III), the magnetization of the present Co-Cu/Cu multilayers consists of a FM and a SPM contribution. The origin of the latter contribution could be assigned to the presence of regions in the magnetic layers which are decoupled from the FM parts and exhibit a SPM behavior. Correspondingly, the observed MR(H) will also be considered as consisting of a MR_{FM} term and GMR_{SPM} contribution.

It has been found that for $H > H_s = 1.7$ kOe the MR(H) curves of the present multilayers could be well described in the form

$$MR(H) = MR_{FM} + GMR_{SPM} L(x), \tag{2}$$

where H_s is the saturation field of the FM magnetization component. For $H > H_s$, the magnetization of all FM regions is completely aligned along the direction of H, and no more change of the MR_{FM} term is expected when increasing H beyond H_s.

According to Eq. (2), the field dependent MR term was found to be proportional to the Langevin function $L(x)$. This is demonstrated in Fig. 3 for the TMR component of strip 2B and similar fits were obtained for all the other MR(H) curves shown in Figs. 2(a) and 2(b). The MR fit results are summarized in Table III where the SPM particle size N_{MR} is derived similarly as N_M in Table II. Within the accuracy of the experimental MR(H) data, the $MR(H) \propto L(x)$ relation gave a reasonably good fit in each case and there was no need to account for a $MR(H) \propto [L(x)]^2$ term as well. Accordingly, the field-dependent part of the magnetoresistance for $H > H_s$ can be identified as the GMR_{SPM} term in the Wiser-Hickey model [case (iii)][36,37] as discussed in Sec. I.

The constant term denoted by MR_{FM} arises due to spin-dependent scattering events in which FM regions are only involved. If two subsequent scattering occurs inside the magnetic layer, there will be a contribution to the AMR effect. If electron scattering happens at the end of a path "FM region $1 \rightarrow$ nonmagnetic region $\rightarrow$ FM region 2" and the magnetization orientation of the two FM regions is not the same, we obtain a contribution to GMR_{FM} [this is term (ii) in the Wiser-Hickey model[36,37] and corresponds to the usual GMR

TABLE III. Magnetoresistance parameters of the multilayer strips investigated. The saturation values of the ferromagnetic (MR_{FM}) and superparamagnetic (GMR_{SPM}) components of the longitudinal (LMR) and transverse (TMR) magnetoresistance as well as parameter N_{MR} characterizing the average cluster size were deduced by fitting the experimental data to Eq. (2). The quantity H_p is half of the separation between the positions of the split MR peaks. Of the H_p values separated by a slash, the first one was determined from the experimental MR curves ($MR_{FM}+GMR_{SPM}$) whereas the second one from the MR_{FM} component only.

Multilayer strip		MR_{FM} (%)	MR_{SPM} (%)	N_{MR}	H_p (Oe) [FM+SPM/FM]
2A	LMR	+0.69±0.08	−0.71±0.07	2140±450	50/50
Co(5.0 nm)/Cu(1.6 nm)	TMR	−0.45±0.04	−1.16±0.02	2630±160	58/65
2B	LMR	+0.25±0.19	−2.51±0.10	2210±330	49/135
Co(4.2 nm)/Cu(2.4 nm)	TMR	−0.46±0.06	−3.02±0.03	1980±70	104/110
3A	LMR	+0.31±0.04	−2.09±0.02	1630±50	90/70
Co(4.6 nm)/Cu(1.9 nm)	TMR	−0.40±0.04	−2.86±0.03	2520±70	93/105
3B	LMR	−0.34±0.05	−4.73±0.02	1790±30	79/105
Co(3.8 nm)/Cu(2.7 nm)	TMR	−0.76±0.07	−5.14±0.03	1900±40	107/131

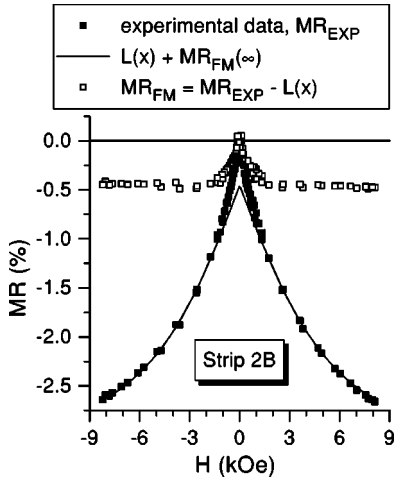

FIG. 3. Demonstration of the separation procedure of the FM and SPM magnetoresistance contributions for multilayer strip 2B. The experimental data for $H>1.7$ kOe are fitted to a Langevin function $L(x)$ which fit yields the GMR_{SPM} term. The MR_{FM} term is obtained by substracting $L(x)$ from the experimental data in the whole range of magnetic field.

contribution in conventional multilayers with completely FM layers only]. For $H>H_s$, both the AMR and the GMR_{FM} terms are constant.

The presence of an AMR term in our multilayers is indicated by the split LMR and TMR curves [see Figs. 2(a) and 2(b)]. It should be noted that the existence of an AMR term gives further evidence that our samples are not granular alloys. In granular systems, the LMR and TMR components are usually indistinguishable since bulklike scattering events leading to AMR cannot occur due to the small size of the magnetic (SPM) regions. In our samples, due to the presence of the AMR term, we can be ascertained about the existence of large FM regions and, therefore, it is justified to assume that the GMR also contains a term corresponding to that typical for conventional multilayers with magnetic layers exhibiting FM behavior only. On the other hand, the presence of FM regions is also a prerequisite for the inclusion of the GMR_{SPM} term and, therefore, the pronounced AMR gives justification also for a treatment in the frame of the Wiser-Hickey model.[36,37]

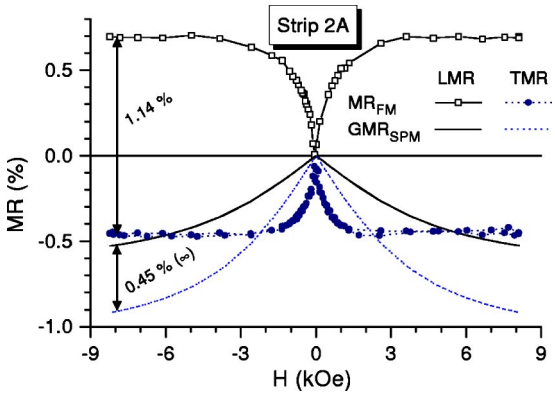

FIG. 4. Decomposed longitudinal and transverse magnetoresistance data for multilayer strip 2A.

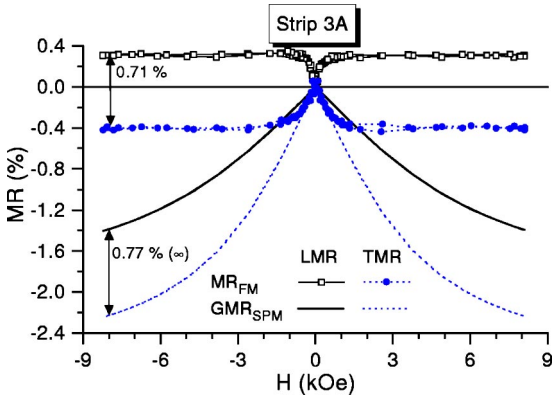

FIG. 5. Decomposed longitudinal and transverse magnetoresistance data for multilayer strip 3A.

When an electron moves in an external electric field to carry a current, it samples randomly and successively all the possible paths leading to spin-dependent scattering events. This is the basis why we can simply add the corresponding MR terms to obtain the total magnetoresistance as was done in Eq. (2).

In viewing the Langevin fit results in Table III, we should keep in mind that the relative weight of the MR_{FM} and the GMR_{SPM} terms as well as that of the two contributions in MR_{FM} (AMR and GMR_{FM}) depend not simply on the volume fractions of the two kinds of magnetic regions but these are also determined by the scattering probability in the different regions as well as other factors related to the mutual spatial distribution and also the morphology of the FM, SPM, and nonmagnetic regions.

The evolution of the MR_{FM} and GMR_{SPM} terms across the multilayer strip series investigated here is displayed in Figs. 4–6 where the results for strip 2B are not shown here since they were very similar to those for strip 3A. The GMR_{SPM} term is negative for both the LMR and the TMR components. This term is the smallest in strip 2A which was previously identified as consisting mainly of percolated FM regions and it is the largest in strip 3B in which the individual magnetic layers are expected to be well separated by nonmagnetic spacer regions (the estimated Cu layer effective thickness is 2.7 nm, see Table I). The MR_{FM} term arising

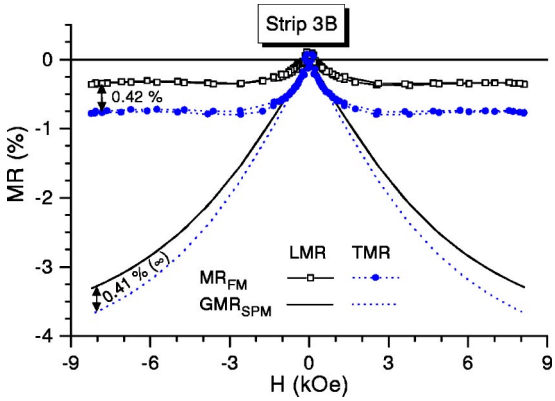

FIG. 6. Decomposed longitudinal and transverse magnetoresistance data for multilayer strip 3B.

from spin-dependent scattering events in which FM regions are only involved is the largest in strip 2A and the smallest in strip 3B. As was discussed above, the MR_{FM} term consists of two contributions: $MR_{FM}=AMR+GMR_{FM}$. Both terms are constant for $H>H_s$ and although the approach to saturation as $H\rightarrow H_s$ certainly follows different functional forms for the AMR and GMR_{FM} contributions, it is hard to predict these functions. Therefore, at the moment there is no way to partition quantitatively the MR_{FM} term into its constituents and we can establish qualitative trends only. For strips 2A, 2B, and 3A, the LMR component of the MR_{FM} term is positive and the TMR component is negative. This indicates that for these three strips the MR_{FM} term is dominated by the AMR component on the account of the GMR_{FM} component. The difference LMR-TMR is especially large for strip 2A, more than half of the AMR of the bulk alloy $Co_{92}Cu_8$ (strip CoB), indicating a large AMR contribution to MR_{FM} for this multilayer strip. This is again expected due to the fact that a large fraction of the FM regions are percolated. On the other hand, for strip 3B both the LMR and the TMR components are negative, indicating that a GMR_{FM} term dominates over the AMR contribution and, indeed, the splitting LMR-TMR is also small here. For strip 3B (Fig. 6) with the largest effective Cu layer thickness (2.7 nm), the magnetic layers are well separated and even the longitudinal component of the MR_{FM} term becomes negative here, indicating a dominance of the GMR_{FM} term over AMR just as expected.

In Table III, the peak positions of both the experimental MR curves and those of the FM component are also included. It is obvious that the H_p value attributed to the FM part is larger than the experimental one when both the FM and SPM components in the MR curves exhibit negative values around $H=0$ (sample 3B, cf. Fig. 6). However, when the LMR component is positive (sample 3A, cf. Fig. 5), the H_p values for that component show the opposite sequence.

The values of N which characterize the average size of the SPM regions as deduced by the Langevin function fit from magnetic measurements (N_M) and from MR data (N_{MR}) are given in Tables II and III, respectively. For a given sample, the agreement of the two N values is reasonably good, they are within a factor of 2 or even much closer. There seems to be a general trend that the N_{MR} values are higher than the N_M values [it is noted that fitting the $MR(H)$ data by $[L(x)]^2$ instead of $L(x)$ roughly doubles the value of N_{MR}, thus further increasing the discrepancy with N_M]. One might actually argue that N_M and N_{MR} should not be necessarily equal. The reason for this may be that there is certainly a distribution of the size of the SPM regions, i.e., of the N values and the two kinds of measurements (magnetization and magnetoresistance) sample differently over this distribution. In the magnetic measurements, the SPM volume fraction is only relevant whereas for MR also the morphology of the SPM regions and their spatial distribution with respect to the FM regions may also play a role not only in the magnitude of the GMR but also in its field dependence.

According to the N_M values in Table I, the typical SPM magnetic moment size in the samples currently investigated is about $1500\mu_B$. This corresponds to approximately 1000 atoms by assuming that in each SPM region about 90% of the atoms is Co with $\mu_{Co}=1.7\mu_B$/atom and 10% is Cu without a magnetic moment. The atomic volumes of Co and Cu in their face centered cubic structure are 0.01113 and 0.01181 nm^3, respectively.[49] By taking 0.0115 nm^3 as the average atomic volume, the typical SPM region size is about 11.5 nm^3. If we think of the SPM regions as magnetically decoupled islands within the plane of the magnetic layers, this corresponds to an island size of about 2 nm $\times$ 2 nm $\times$ 3 nm whereby we assumed an island thickness of 3 nm which is slightly less than the actual average magnetic layer thickness (4 nm, see Table I). One can also visualize the SPM regions as a chemically intermixed interfacial layer of, say, 0.6 nm thickness corresponding to about three atomic layers. This picture leads to about 4 nm $\times$ 5 nm as the lateral dimensions of an average SPM region in the form of an intermixed interface. It should be mentioned that even if we take the typical SPM magnetic moment size as about $2000\mu_B$ due to the larger N_{MR} values in Table III, the lateral SPM region sizes increase by about 1 nm only for both the islands and the intermixed interfaces. It is emphasized, however, that the above figures for the characteristic SPM sizes are rough estimates only. Evidently, detailed sophisticated structural and chemical analysis techniques will be required to establish the actual size and morphology of the SPM regions. However, should one acquire detailed information on the spatial distribution and morphology of the three constituent phases (FM, SPM, and nonmagnetic regions), it will not be a straightforward task even in that case to predict the magnitude of the individual MR contributions these magnetic nanostructures.

V. SUMMARY AND CONCLUSIONS

In the present work, both the magnetization and the magnetoresistance were decomposed into a FM and a SPM term for multilayers with strongly nonsaturating MR behavior. The separation of the MR componets was performed on the basis of the Wiser-Hickey model[36,37] elaborated for granular alloys with the simultaneous presence of both FM and SPM particles. In such a case this model predicts that conduction electron paths "FM region 1 $\rightarrow$ nonmagnetic region $\rightarrow$ SPM region 2" (or in the reverse sequence) lead to the relation $MR(H)\propto L(x)$.[36,37]

It was shown in the present paper that in multilayers with a significant SPM magnetization contribution the field dependence of the magnetoresistance can also be described as $MR(H)\propto L(x)$ for magnetic fields beyond the saturation field (H_s) of the FM component. The size of the SPM regions as deduced from the MR data for the electrodeposited Co-Cu/Cu multilayers investigated was very close to those obtained from the magnetic measurements. By this analysis, we could separate for $H>H_s$ the observed MR into two contributions: a constant MR_{FM} term from scattering events in which FM regions only are involved and the above described term denoted by GMR_{SPM} which arises due to the simultaneous presence of both FM and SPM regions. The MR_{FM} term is composed of an anisotropic magnetoresistance contribution and the conventional multilayer GMR effect which cannot be separated from each other at present. From the lack of the $MR(H)\propto[L(x)]^2$ term, we can furthermore con-

clude that the SPM regions which are magnetically decoupled from the FM regions are separated from the next SPM regions by FM regions in every directions. The typical SPM size in the samples studied was estimated to be about 2 nm × 2 nm × 3 nm in the form of separated islands or 4 nm × 5 nm × 0.6 nm in the form of about 3 atomic layer thick chemically intermixed interfaces.

An evaluation of the MR curves and their evolution with temperature for several electrodeposited Co-Cu/Cu, Fe-Co-Cu/Cu, and Co-Ni-Cu/Cu multilayer series by the method presented in this paper is in progress. It is believed that an analysis as described here will help to reveal in general how the specific multilayer deposition conditions control the magnitude, the field dependence and the field sensitivity of GMR in multilayers via microstructure evolution. It has to be mentioned that the GMR analysis method described above is applicable for multilayers regardless of the specific deposition technique.

ACKNOWLEDGMENT

This work was supported by the Hungarian Scientific Research Fund (OTKA) through Grant No. T037673.

*Email address: bakonyi@szfki.hu

†Undergraduate student at Eötvös University, Budapest during the course of this work.

[1] M. Alper, K. Attenborough, R. Hart, S.J. Lane, D.S. Lashmore, C. Younes, and W.S. Schwarzacher, Appl. Phys. Lett. **63**, 2144 (1993).

[2] M. Alper, K. Attenborough, V. Baryshev, R. Hart, D.S. Lashmore, and W. Schwarzacher, J. Appl. Phys. **75**, 6543 (1994).

[3] D. Barlett, F. Tsui, D. Glick, L. Lauhon, T. Mandrekar, C. Uher, and R. Clarke, Phys. Rev. B **49**, 1521 (1994).

[4] R. Clarke, D. Barlett, F. Tsui, B.X. Chen, and C. Uher, J. Appl. Phys. **75**, 6174 (1994).

[5] K. Attenborough, R. Hart, S.J. Lane, M. Alper, and W.S. Schwarzacher, J. Magn. Magn. Mater. **148**, 335 (1995).

[6] S.K.J. Lenczowski, C. Schönenberger, M.A.M. Gijs, and W.J.M. de Jonge, J. Magn. Magn. Mater. **148**, 455 (1995).

[7] J. Xu, M.A. Howson, B.J. Hickey, D. Greig, P. Veillet, and E. Kolb, J. Magn. Magn. Mater. **156**, 379 (1996).

[8] M. Nawate, M. Itogawa, and S. Honda, J. Magn. Magn. Mater. **156**, 383 (1996).

[9] T. Sugiyama and O. Nittono, J. Magn. Magn. Mater. **156**, 143 (1996).

[10] I. Bakonyi, E. Tóth-Kádár, T. Becsei, J. Tóth, T. Tarnóczi, Á. Cziráki, I. Gerőcs, G. Nabiyouni, and W. Schwarzacher, J. Magn. Magn. Mater. **156**, 347 (1996).

[11] M. Alper, W. Schwarzacher, and S.J. Lane, J. Electrochem. Soc. **144**, 2346 (1997).

[12] T. Lucinski, F. Stobiecki, D. Elefant, D. Eckert, G. Reiss, B. Szymanski, J. Dubowik, M. Schmidt, H. Rohrmann, and K. Roell, J. Magn. Magn. Mater. **174**, 192 (1997).

[13] J. Tóth, L.F. Kiss, E. Tóth-Kádár, A. Dinia, V. Pierron-Bohnes, and I. Bakonyi, J. Magn. Magn. Mater. **198–199**, 243 (1999).

[14] E. Tóth-Kádár, L. Péter, T. Becsei, J. Tóth, L. Pogány, T. Tarnóczi, P. Kamasa, I. Bakonyi, G. Láng, Á. Cziráki, and W. Schwarzacher, J. Electrochem. Soc. **147**, 3311 (2000).

[15] F. Spizzo, E. Angeli, D. Bisero, P. Vavassori, and F. Ronconi, Appl. Phys. Lett. **79**, 3293 (2001).

[16] L. Péter, Á. Cziráki, L. Pogány, Z. Kupay, I. Bakonyi, M. Uhlemann, M. Herrich, B. Arnold, T. Bauer, and K. Wetzig, J. Electrochem. Soc. **148**, C168 (2001).

[17] F. Spizzo, E. Angeli, D. Bisero, P. Vavassori, and F. Ronconi, J. Magn. Magn. Mater. **242–245**, 473 (2002).

[18] M. Shima, L.G. Salamanca-Riba, R.D. McMichael, and T.P. Moffat, J. Electrochem. Soc. **149**, C439 (2002).

[19] G. Nabiyouni, W. Schwarzacher, Z. Rolik, and I. Bakonyi, J. Magn. Magn. Mater. **253**, 77 (2002).

[20] I. Bakonyi, J. Tóth, L. Goualou, T. Becsei, E. Tóth-Kádár, W. Schwarzacher, and G. Nabiyouni, J. Electrochem. Soc. **149**, C195 (2002).

[21] P. Vavassori, F. Spizzo, E. Angeli, D. Bisero, and F. Ronconi, J. Magn. Magn. Mater. **262**, 120 (2003).

[22] V. Weihnacht, L. Péter, J. Tóth, J. Pádár, Zs. Kerner, C.M. Schneider, and I. Bakonyi, J. Electrochem. Soc. **150**, C507 (2003).

[23] I. Bakonyi, J. Tóth, L.F. Kiss, E. Tóth-Kádár, L. Péter, and A. Dinia, J. Magn. Magn. Mater. **269**, 156 (2004).

[24] W.R.A. Meuleman, S. Roy, L. Péter, and I. Bakonyi, J. Electrochem. Soc. **151**, C256 (2004).

[25] Q.X. Liu, L. Péter, J. Tóth, L.F. Kiss, Á. Cziráki, and I. Bakonyi, J. Magn. Magn. Mater. **280**, 60 (2004).

[26] S.S.P. Parkin, N. More, and K.P. Roche, Phys. Rev. Lett. **64**, 2304 (1990).

[27] D.H. Mosca, F. Petroff, A. Fert, P.A. Schroeder, W.P. Pratt, Jr., and R. Laloee, J. Magn. Magn. Mater. **94**, L1 (1991).

[28] H. Kubota, S. Ishio, T. Miyazaki, and Z.M. Stadnik, J. Magn. Magn. Mater. **129**, 383 (1994).

[29] J. Xu, M.A. Howson, B.J. Hickey, D. Greig, E. Kolb, P. Veillet, and N. Wiser, Phys. Rev. B **55**, 416 (1997).

[30] M. Wu and W. Abdul-Razzaq, Phys. Rev. B **42**, 4590 (1990).

[31] B.D. Cullity, *Introduction to Magnetic Materials* (Addison-Wesley, Reading, 1972).

[32] J.L. Gittleman, Y. Goldstein, and S. Bozowski, Phys. Rev. B **5**, 3609 (1972).

[33] S. Zhang, Appl. Phys. Lett. **61**, 1855 (1992).

[34] J.Q. Xiao, J.S. Jiang, and C.L. Chien, Phys. Rev. Lett. **68**, 3749 (1992).

[35] C.L. Chien, Mater. Sci. Eng., B **31**, 127 (1995).

[36] N. Wiser, J. Magn. Magn. Mater. **159**, 119 (1996).

[37] B.J. Hickey, M.A. Howson, S.O. Musa, and N. Wiser, Phys. Rev. B **51**, 667 (1995).

[38] B.J. Hickey, M.A. Howson, S.O. Musa, G.J. Tomka, B.D. Rainford, and N. Wiser, J. Magn. Magn. Mater. **147**, 253 (1995).

[39] J. Xu, B.J. Hickey, M.A. Howson, D. Greig, R. Cochrane, S. Mahon, C. Achilleos, and N. Wiser, Phys. Rev. B **56**, 14 602 (1997).

[40] N. Wiser, Philos. Mag. B **77**, 1263 (1998).

[41] W.R.A. Meuleman, S. Roy, L. Péter, and I. Varga, J. Electrochem. Soc. **149**, C479 (2002).
[42] L. Péter, Q.X. Liu, Zs. Kerner, and I. Bakonyi, Electrochim. Acta **49**, 1513 (2004).
[43] M. Prutton, *Thin Ferromagnetic Films* (Butterworths, London, 1964).
[44] M. Cerisier, K. Attenborough, J.-P. Celis, and C. Van Haesendonck, Appl. Surf. Sci. **166**, 154 (2000).
[45] I.A. Campbell and A. Fert, in *Ferromagnetic Materials*, edited by E.P. Wohlfarth (North-Holland, Amsterdam, 1982).
[46] R.M. Bozorth, *Ferromagnetism* (Van Nostrand, New York, 1951), Vol. 3, Chap. 9.
[47] T.R. McGuire and R.I. Potter, IEEE Trans. Magn. **11**, 1018 (1975).
[48] I. Bakonyi, E. Tóth Kádár, J. Tóth, L.F. Kiss, L. Pogány, Á. Cziráki, C. Ulhaq-Bouillet, V. Pierron-Bohnes, A. Dinia, B. Arnold, and K. Wetzig, Europhys. Lett. **58**, 408 (2002).
[49] P. Villars and L.D. Calvert, *Pearson's Handbook of Crystallographic Data for Intermetallic Phases* (American Society of Metals, Metals Park, Ohio, 1985).